

Original papers

Predictive model based on artificial neural network for assessing beef cattle thermal stress using weather and physiological variables

Rafael Vieira de Sousa, Alex Vinicius da Silva Rodrigues, Mariana Gomes de Abreu, Rubens Andre Tabile, Luciane Silva Martello*

Department of Biosystems Engineering, Faculty of Animal Science and Food Engineering (FZEA), University of São Paulo (USP), Av. Duque de Caxias Norte, 225, Pirassununga, SP ZIP 13635-900, Brazil

ARTICLE INFO

Keywords:

Precision livestock farming
Soft computing
Thermal radiation
Animal welfare
Non-invasive measurement

ABSTRACT

The performance of feedlot cattle is adversely affected by thermal stress but the approach to assess the status of animal stress can be laborious, invasive, and/or stressful. To overcome these constraints, the present study proposes a model based on an artificial neural network (neural model), for individual assessment of the level of thermal stress in feedlot finishing cattle considering both weather and animal factors. An experiment was performed using two different groups of Nellore cattle. Physiological and weather data were collected during both experiments including surface temperatures for four selected spots, using infrared thermography (IRT). The data were analyzed (in terms of Pearson's correlation) to determine the best correlation between the weather and physiological measurements and the IRT measurements for defining the best body location and physiological variable to support the neural model. The neural model had a feed-forward and multi-layered architecture, was trained by supervised learning, and accepted IRT, dry bulb temperature, and wet bulb temperature as inputs to estimate the rectal temperature (RT). A regression model was built for comparison, and the predicted and measured RTs were classified on levels of thermal stress for comparing with the classification based on the traditional temperature–humidity index (THI). The results suggested that the neural model has a good predictive ability, with an R^2 of 0.72, while the regression model yielded R^2 of 0.57. The thermal stress predicted by the neural model was strongly correlated with the measured RT (94.35%), and this performance was much better than that of the THI method. In addition, the neural model demonstrated good performance on previously unseen data (ability to generalize), and allowed the individual assessment of the animal thermal stress conditions during the same period of day.

1. Introduction

The performance of feedlot cattle is negatively affected by high ambient temperatures, humidity, and solar radiation, which reduce the dry matter intake, increase the body temperature, and decrease the weight gain (Mader and Griffin, 2015). Previous research demonstrated a strong correlation between weather variables and animal welfare, assessed in terms of physiological responses such as body temperature (Mader, 2006; Burfeind et al., 2012; Gaughan and Mader, 2013). However, the approach to assessing the animal status traditionally includes manual and visual scoring, which is laborious, invasive, and imposes stress on the tested animals (Wathes et al., 2008).

Some indices of thermal stress based on environmental variables have been proposed (Dikmen and Hansen, 2009). One of the most used in research is the temperature–humidity index (THI) (Thom, 1959).

However, the THI does not consider the individual responses of animals and breed (Eigenberg et al., 2005; Da Silva et al., 2007; Dikmen and Hansen, 2009). Furthermore, the animal thermal stress is a result of thermal energy exchange between the animals and their environment, and depends on both physiological and environmental factors (Taylor et al., 1969; Collier et al., 2006; Mader and Griffin, 2015). Thus, development of models that use non-invasive input data for predicting the thermal stress that consider, in addition to environmental factors, the physiological response of the animal, can contribute more adequately to assessment of the animal health and welfare. Such methods are likely to contribute to novel decision making systems for increasing livestock productivity and efficiency of resource involved in livestock production (Scharf et al., 2011; Dikmen and Hansen, 2009; Martello et al., 2015).

The blood flow to the surface of the skin is an important regulator of heat exchange. Animal temperature in the superficial layers of skin can

* Corresponding author.

E-mail addresses: rafael.sousa@usp.br (R.V.d. Sousa), alex.rodrigues@usp.br (A.V.d.S. Rodrigues), mariana.abreu@usp.br (M.G.d. Abreu), tabile@usp.br (R.A. Tabile), martello@usp.br (L.S. Martello).

<https://doi.org/10.1016/j.compag.2017.11.033>

Received 18 August 2017; Received in revised form 16 November 2017; Accepted 22 November 2017

0168-1699/© 2017 Elsevier B.V. All rights reserved.

be used for diagnosing inflammatory processes that are accompanied by changes in the peripheral blood circulation, thus affecting local and general thermal equilibria (Metzner et al., 2014). Motivated by this notion, instrumentation systems that use infrared thermography (IRT) have been considered for monitoring body surface temperature profiles and their relationship to other animal welfare traits (Wathes et al., 2008). Montanholi et al. (2008) studied the correlation between the IRT-measured temperature of different body surface areas and heat and methane production in dairy cows. Montanholi et al. (2009) demonstrated the potential application of IRT in the assessment of feed efficiency in beef bulls. A non-invasive and automated method was suggested by Schaefer et al. (2012) for the identification of the bovine respiratory disease in receiver calves, using IRT. Metzner et al. (2014) compared different algorithms for the evaluation of udder skin thermography images for the detection of acute mastitis and fever, seeking to obtain objective and valid results for future automated computer-supported processing. Martello et al. (2015) evaluated the use of IRT images as a tool for monitoring the body surface temperature of beef cattle, and its relationship to residual feed intake.

Mathematical models are frequently generated to merge several input data and predicting some specific responses from a dynamic system. In a typical biological system, its component subsystems, such as the animal thermoregulation system, and the complex interactions between them, introduce a large number of variables, which results in rather complex mathematical modelling. Recently, some predictive modelling methods based on soft computing techniques have been used for assessment of animal welfare using non-invasive sensors integrated into predictive models (Huang et al., 2010; Sousa et al., 2016). Brown-Brandl et al. (2005) designed and evaluated five different models for predicting thermal stress in cattle: two statistical models, two fuzzy inference systems, and one artificial neural network (ANN). Among these, the ANN-based method yielded the best results. Shao and Xin (2008) considered a real-time image processing system for the detection of motion and classification of the thermal stress state of group-housed pigs, based on their resting behavioral patterns. Hernandez-Julio et al. (2014) evaluated techniques for modelling the physiological responses, rectal temperature (RT), and respiratory rate of black and white Holstein dairy cows. Again, the model based on the ANN demonstrated the best performance, followed by the models based on neuro-fuzzy networks and regression. Sousa et al. (2016) proposed a fuzzy classifier that yielded better estimates of the thermal stress level, compared with the traditional THI and previously considered fuzzy-based systems.

This paper continues the approach presented by Sousa et al. (2016) for developing a non-invasive method for prediction of physiological variables related to the thermal stress state of cattle. The objective of this study was to develop and test an ANN-model to provide a prediction of animal thermal stress state using surface temperature and weather data.

2. Materials and methods

The proposed model based on ANN (neural model) for predicting physiological variables was developed and tested on two different groups of Nellore finishing cattle confined in two phases (two feedlots) for data collection. The data collected should broadly cover the problem domain including exceptions and conditions within the boundaries of the problem domain. In this sense, different numbers of animals (first phase $n = 8$, second phase $n = 18$) and data collection schemes were used applied for each group, for increasing the data heterogeneity for the ANN training. In both phases, the acquired physiological data included rectal temperature (RT), respiration rate (RR), and body surface temperature (IRT) from four body locations detailed in Sousa et al. (2016): front, ocular area, flank, and front feet. In addition, the weather data of the dry bulb temperature (DBT) and wet bulb temperature (WBT) were stored and used in modelling.

Before constructing the neural model, a statistical analysis based on

Pearson's correlation was performed on the IRT data from different body locations (front, ocular area, flank and front feet) and physiological variables (RT and RR), to determine the best body location and physiological variable to use in the predictive model. The results of this statistical analysis are detailed in Sousa et al. (2016), who used the same groups of animals to develop a fuzzy logic-based predictive model.

After the data were collected and analyzed, the neural model was designed, trained, and modified as needed, for yielding accurate results. A regression model was built for comparison. The final models that were built were then run against the selected test data to generate predictions, calculate linear correlations between the measured and estimated animal responses, and evaluate the models' predictive abilities. In addition, the predicted RT (PRT) was rated for the level of thermal stress (thermal stress classification) and compared with the classification of thermal stress based on the measured RT and on the traditional THI.

2.1. Data acquisition and statistical analysis

The experiments were conducted between May (first phase) and July (second phase), 2010, at the facilities of the Faculty of Animal Science and Food Engineering (FZEA) of the University of São Paulo (USP) in Pirassununga, SP, Brazil, located at 21°57'02"S, 47°27'50"W, at a mean elevation of 630 m above the sea level. The average annual temperature in that region is 22.00 °C, with approximately 1360 mm of rain per year. In the first phase, the average temperature and relative humidity were 23.80 ± 0.37 °C (range 8.80–31.60 °C) and $70.00 \pm 1.31\%$ (range 40.00–96.10%), respectively. In the second phase, these parameters were 26.40 ± 0.15 °C (range 18.60–29.60 °C) and $39.70 \pm 0.47\%$ (range 23.90–74.90%), respectively.

The experiments were regulated according to the Institutional Animal Care and Use Committee Guidelines of FZEA/USP. The physiological data in both phases were collected daily with the cattle restrained in the squeeze chute over the shade (around 10 min), using the same tools. In the first phase, eight Nellore steers (18 month-old, 380 ± 15 kg initial body weight, and castrated) were evaluated over a period of eight days. In the second phase, eighteen Nellore steers (16–21 month-old, 334 ± 19 kg initial body weight, and castrated) were evaluated over a period of ten days. For both phases the cattle were allotted in individual pens and were exposed to natural environmental conditions. The cattle were housed in individual pens (5 × 8 m) with soil-surface, automatic water fountains and sheltered feed bunks, fed ad libitum diet.

In the first phase the measurements of RT, RR, and IRT were collected for all cattle at 7 a.m., 11 a.m., 2 p.m., and 4 p.m. In the second phase ($n = 18$) the same variables were measured at 7 a.m., 12 a.m., and 4 p.m. The RT was collected manually, using a digital thermometer (VMDT01, Viomed, China). The RR was measured by counting the flank movements within a period of 15 s, and the measurements were repeated three times for obtaining an average RR for the period. The IRT images were acquired using a thermographic camera (TI 20-9 Hz, Fluke Corporation, Everett, USA) with the emissivity of 0.98, at a distance of approximately 1 m from each of the four body locations (front, ocular area, flank, and front feet). The WBT and DBT data were stored using a data logger (HOBO U12, Onset Computer Corporation, USA) that was fixed at the center of the pens at 2 m above the floor, approximately at the level of the cattle head. These weather variables were automatically recorded 24 h a day, with hourly intervals. Additional details about the animals, the feeding, the facilities and the physiological data collected are described in Sousa et al. (2016).

Before performing the statistical analysis, the data (IRT, RR, TR, DBT, WBT) from measurements associated to low quality images were manually eliminated. The images were interpreted using the software FLUKE InsideIRTM 4.0 (FLUKE Corporation, EUA) and it was obtained the average temperatures for the front, flank, and front feet areas, and

Table 1
Correlations (r) between infrared temperature traits of different body parts (IRT), physiological variables (RT and RR) and weather variables (DBT and WBT).

Traits	r _{DBT} (p value)	r _{WBT} (p value)	r _{RT} (p value)	r _{RR} (p value)
IRT – Front	0.97 (0.0001)	0.86 (0.0001)	0.79 (0.0001)	0.63 (0.0001)
IRT – Eyes	0.92 (0.0001)	0.80 (0.0001)	0.77 (0.0001)	0.55 (0.0001)
IRT – Feet	0.95 (0.0001)	0.83 (0.0001)	0.72 (0.0001)	0.60 (0.0001)
IRT – Flank	0.93 (0.0001)	0.85 (0.0001)	0.76 (0.0001)	0.63 (0.0001)

the maximal temperature for the ocular area. Overall, 796 measurements were analyzed (256 in the first phase and 540 in the second phase). Thirty-three thermographic images from the first phase were discarded owing to their low quality that would be translated into low-accuracy temperature data.

The statistical analysis based on Pearson’s correlation was performed for IRT data for different body locations (front, ocular area, flank and front feet) and physiological variables (RT and RR). All analyses were performed using the SAS System software 9.3 (SAS Institute Inc., Cary, NC, USA), and the procedures and results are detailed in Sousa et al. (2016). Table 1 summarizes the main findings.

The study of Sousa et al. (2016) found that the correlation between the RT and weather variables was stronger than that between the RR and weather variables. In addition, considering all IRT traits, the study found that the front temperature was strongly correlated with DBT (0.97), WBT (0.86), and RT (0.79); these findings are summarized in Table 1.

In the present work, following the conclusions of Sousa et al. (2016), the RT was chosen as the output (dependent) variable of the neural model, while the IRT of the front (Fig. 1), DBT, and WBT served as the input (independent) variables to the neural model. The IRT traits defined in this study were the average temperature of a specific shape (rectangle of 65 × 139 pixels) of the front area (Fig. 1) to define a sub-area of each image. Through the tool box of the IRT software this sub-area (same shape and size) was used for all other front images.

Previous studies (Kessel et al., 2010; Mccafferty, 2007; Weschenfelder et al., 2013) considered regions of the head (i.e., brain)

as an indicator of core temperature because of its proximity to the brain, which houses the central nervous system and is responsible for body temperature regulation.

2.2. Neural network model

The neural model was implemented using the Neural Network Toolbox in MATLAB R2010b software (Mathworks Inc., USA), according to the fitting methodology. The neural network model had a feed-forward and multi-layered architecture, with a sigmoid transfer function in the hidden layer and a linear transfer function in the output layer. The neural architecture was run (simulated) in several realizations, to fine-tune the neural network’s parameters using the supervised learning approach. The neural network accepted DBT, WBT, and front IRT as inputs, and estimated the RT output (PRT) for given input parameters. For training the neural network, it was used 60% of the data randomly selected (typical value find in literature and confirmed on fine-tune procedure – 70% and 60% are the most common). The training was performed using the Levenberg–Marquardt back-propagation method, the mean squared error was used as a measure of performance, the learning rate was 0.01, the performance goal was 0.00, and maximum of 1000 iterations were used for learning. The remaining 40% of the data were partitioned into a validation set (20%) and test set (20%).

Different ANNs were considered, with the number of neurons (N) in the hidden layer set to 7, 10, 15, 20, 30, 50, and 100. In addition, as the input data were randomly selected, the performance of the model could be affected by the specific dataset chosen for training. Thus, choosing less representative data for training is likely to yield a less generalizable model. Thus, it was trained one hundred neural networks for each hidden layer architecture, with different random partitions of the data across different realizations. Fig. 2 shows the flowchart of the algorithm for training an ensemble of ANNs.

As Fig. 2 shows, for each hidden layer architecture the algorithm determined the best ANN out of one hundred realizations. Thus, overall seven hundred ANNs were generated and compared, and one ANN was selected for each hidden layer architecture (totaling seven

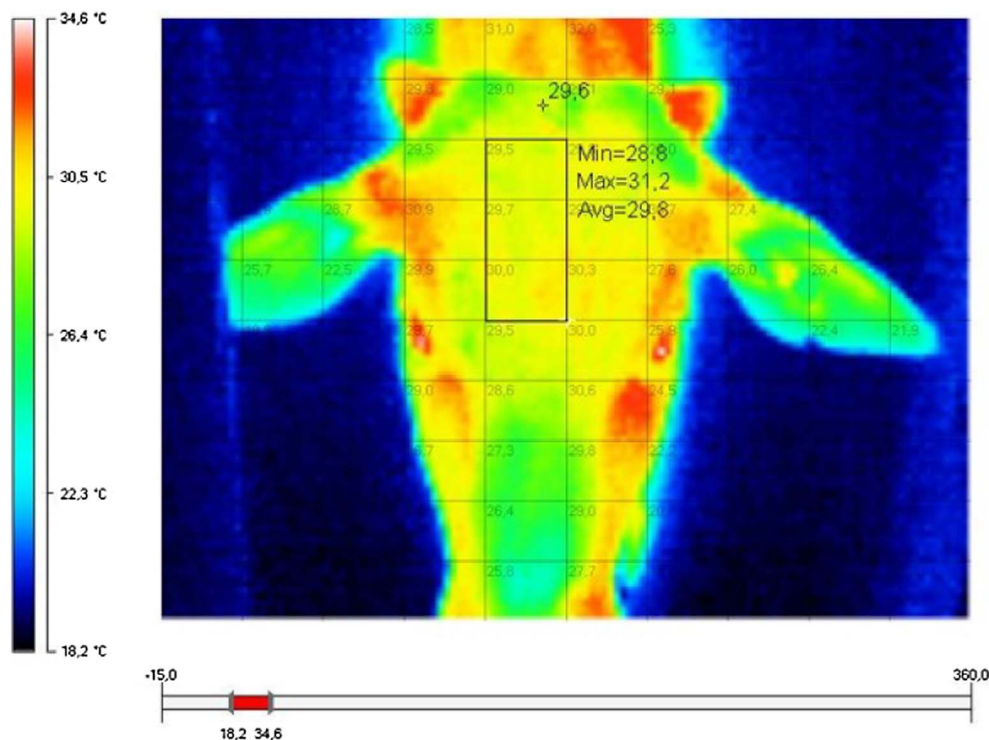


Fig. 1. Illustrative infrared images of the front and the specific shape (rectangle) of the body location used for deriving the infrared temperatures.

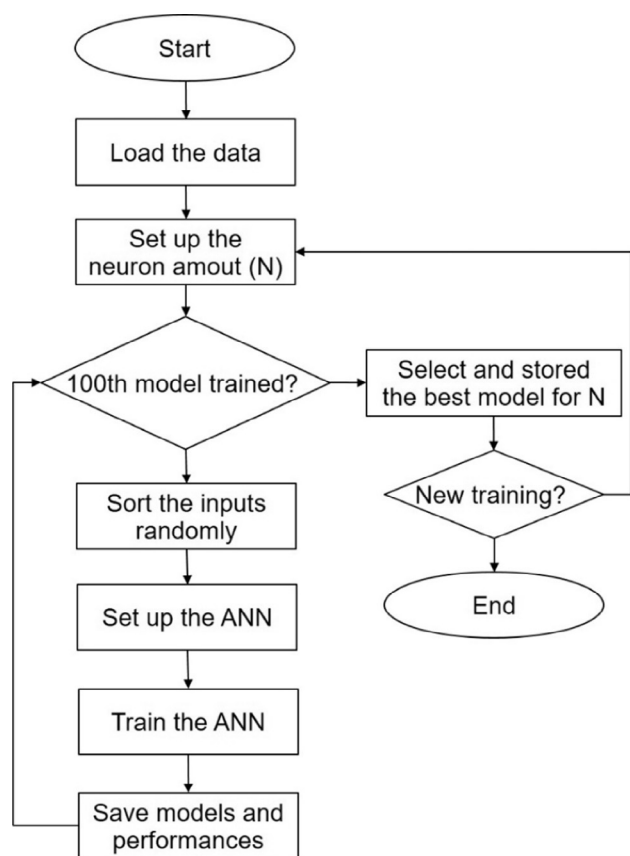


Fig. 2. Flowchart of the algorithm for determining the best neural model.

architectures). The performance of these ANNs was evaluated by comparing the PRTs and measured RTs using the linear regression model and its parameters – the slope, the intercept, the mean error, the root mean square error (RMSE), and the determination coefficient (R^2).

2.3. Classical regression-based modelling

The best-performing ANN was selected and compared with a linear regression model. The regression model was fit using the regression routine in the SAS software 9.3 (SAS Institute Inc., Cary, NC, USA). The same datasets (60% for training, 20% for validation, and 20% for testing) as those that were used for training and selecting the best ANN were used for training, validating, and testing the regression model. The regression model was parameterized in terms of its statistical parameters – the slope, the intercept, the mean error, the RMSE, and R^2 .

2.4. Evaluation and validation of the classifier

The models were also evaluated in terms of the thermal stress classification on the measured RT, the RT predicted by the ANN, and the classification obtained using the traditional THI that was proposed by Thom (1959). The THI was determined for every time interval, as follows:

$$THI = 0.72(DBT + WBT) + 47 \tag{1}$$

The measured and predicted RT values were classified into four categories: normal, alert, danger, and emergency. The RT thresholds that were used in the present study to classify into different heat stress levels were based on those used by Kolb (1987) and are listed in Table 2. The THI thresholds were the same as those adopted by the Livestock Weather Safety Index (Thom, 1959; Eigenberg et al., 2005), which categorizes the heat stress level also showed in Table 2.

Table 2
Rectal temperature (RT) and temperature-humidity (THI) index based classification of the levels of heat stress of beef cattle.

Levels of Thermal Stress	RT (°C)	THI
Normal	RT < 39.1	THI ≤ 74
Alert	39.1 ≤ RT < 39.5	74 < RT ≤ 79
Danger	39.5 ≤ RT < 40.5	79 < RT ≤ 84
Emergency	RT ≥ 40.5	THI > 84

The frequency distribution and coincidence (%) were used to summarize the distribution of values in the different categories and to allow a comparative analysis between the levels of thermal stress which correspond to the THI, ANN, and the measured RT. This methodology (comparative analysis) was applied for all data obtained in both experimental phases.

3. Results and discussion

The results are shown in the following sequence. First, it is described the best ANN considering the number of neurons in the hidden layer and the input data. Next, it is presented the regression model obtained for the same training data that yielded the best ANN. The thermal stress ratings based on the measured RTs and PRTs are shown and compared with the THIs. Finally, the results are discussed and compared with results of some previous studies.

3.1. Neural model

The statistical parameters related to the seven best models (with seven different hidden layer configurations) obtained at the completion of the training process are listed in Table 3. All of the parameters in Table 3 are significant, with $p < 0.001$.

Considering the mean error, the RMSE, and R^2 in Table 3, the three best models were those that had 50, 75, and 100 neurons in their hidden layers. The best performing model was the one with 50 neurons for which the mean error was 0.21 °C and the RMSE was 0.27 °C. This model was able to account for 73% of total variation in RT. In this case, the slope was 0.95 and the intercept was 1.78.

The statistical parameters related to the seven best models tested against the remaining 20% of data are presented in Table 4 (all of the parameters are significant, with $p < 0.001$).

Similar to the results for the training set, the best-performing ANN in Table 4 was the one with 50 neurons in the hidden layer. This neural network accounted for 72% of total variation in RT. In this case, the mean error was 0.23 °C, the RMSE was 0.28 °C, the slope was 0.88, and the intercept was 4.60. Correspondence between the measured RT and that predicted by the best ANNs is shown in Fig. 3a and b, for the training set and test set data, respectively.

3.2. Regression model

The linear regression model was obtained for the same training set data (60%) that were used for determining the best ANN. The statistical parameters of the linear regression model are listed in Table 5.

Using from the parameters of the linear regression parameters in Table 5, the following linear model was generated:

$$TR = 0.04289 DBT - 0.02856 WBT + 0.05988 IRT + 35.87991 \tag{2}$$

Here, the total RT variation is 53.33% and all parameters are statistically significant ($p < 0.001$). The distribution of RT-related variation was accounted for by the DBT (49.60%), WBT (1.79%), and IRT (1.94%).

Linear relationships between the measured RT and PRT (linear regression) were obtained for both the training set data and the test set data. The statistical parameters related to the performances of the

Table 3
Statistical results for the seven models with different hidden layer architectures, for simulations on the training set data.

	N = 7	N = 10	N = 15	N = 20	N = 30	N = 50	N = 75	N = 100
Slope	1.02	1.02	1.03	0.98	0.94	0.95	0.98	0.93
Intercept	-0.93	-0.73	-1.20	0.72	2.34	1.78	0.87	2.58
Mean Error, °C	0.23	0.23	0.24	0.23	0.24	0.21	0.22	0.21
RMSE, °C	0.31	0.30	0.31	0.31	0.31	0.27	0.29	0.28
R ²	0.66	0.67	0.64	0.66	0.66	0.73	0.69	0.72

N, number of neurons; RMSE, root mean square error; R², coefficient of determination.

linear regression model on these data sets are listed in Table 6 (all of the parameters are significant, with $p < 0.001$). Fig. 4a and b show the correspondence between the measured RT and PRT using the linear regression model, for both the training set data and test set data.

3.3. Assessing the thermal stress

To assess the predictive ability of the ANN model for thermal stress classification in cattle, the RTs predicted by the ANN model were classified into levels of thermal stress according to Table 2, and this classification was compared with a similar classification based on the measured RTs and THIs (Tables 7 and 8).

Table 7 shows that the THI-based and ANN-based RT classifications agreed only in 31.91% of cases (31.66% agreement on “normal”, 0.25% agreement on “alert”, 0% agreement on “danger”, and 0% agreement on “emergency”). The THI-based classification agreed with the measurement-based RT classification only in 33.17% of cases (31.66% agreement on “normal”, 1.51% agreement on “alert”, 0% agreement on “danger”, and 0% agreement on “emergency”).

The comparison between predicted and measured RT assessments (Table 8) reveals that the two methods agreed in 94.35% of cases (93.97% agreement on “normal”, 0.38% agreement on “alert”, 0% agreement on “danger”, and 0% agreement on “emergency”). Just as in the case of measurement-based RT classification, prediction-based RT classification classified no measures as “emergency”. In addition, prediction-based RT classification appears to have slightly underestimated the “danger” and “alert” categories, classifying some of these measures as “alert” and “normal”, respectively.

3.4. Discussion

Comparing the data in Table 4 and Table 6, it is possible to evaluate the performance of the ANN model (with 50 neurons in the hidden layer) and the regression model, on the test set data. The superior performance of the ANN was verified. For the ANN, the mean error and the RMSE were 0.23 °C and 0.28 °C, respectively, while for the regression model those measures were 0.28 °C and 0.34 °C, respectively. In addition, the R² value for the ANN model was 0.72 (Table 4); consequently, the value of r was 0.85 (Fig. 3b). Both of these measures had higher values than those obtained for the regression model, which yielded R² of 0.57 (Table 6) and r of 0.75 (Fig. 4b). Thus, compared with the regression model the RT estimates generated by the ANN model are much stronger correlated with the actually measured values.

Table 4
Statistical results for the seven models with different hidden layer architectures, for simulations on the test set data.

	N = 7	N = 10	N = 15	N = 20	N = 30	N = 50	N = 75	N = 100
Slope	1.04	1.07	1.05	0.95	0.91	0.88	0.93	0.83
Intercept	-0.16	-2.82	-2.08	1.73	3.49	4.60	2.57	6.70
Mean Error, °C	0.25	0.25	0.26	0.26	0.25	0.23	0.23	0.26
RMSE, °C	0.32	0.32	0.33	0.34	0.32	0.28	0.29	0.33
R ²	0.66	0.65	0.66	0.68	0.71	0.72	0.69	0.67

N, number of neurons; RMSE, root mean square error; R², coefficient of determination.

According to the results for the training set data (Fig. 3a), the ANN model yielded a significantly higher coefficient correlation (0.86, corresponding to R² = 0.74) compared with the results obtained by Sousa et al. (2016) (0.71, corresponding to R² = 0.50). Sousa et al. (2016) developed and validated a fuzzy logic-based predictive model that used the same inputs for estimating RT.

The statistical results for the test set data, presented in Table 4, can be used for comparing the performance of the ANN model with performances of similar models proposed by other authors. In Brown-Brandl et al. (2005), five types of inputs were used (one of which was the cattle breed and the other four were weather variables) to estimate the RR. Those authors used a similar ANN architecture as the one proposed in this work, but with a larger number of inputs, 12 neurons in the hidden layer, and with a different training process. When simulated on the test set data (30% of the overall data set) to estimate the RR, the model proposed by Brown-Brandl et al. (2005) yielded R² of 0.68 and mean error of 1.04 °C, while for the ANN model in the present work the values of those same parameters were 0.72 and 0.23 °C, respectively (Table 4).

Hernandez-Julio et al. (2014) developed two neural models that used two weather variables to estimate the RR and RT for Holstein dairy cows. The authors used a similar ANN architecture as the one used in the present work; however, the training process was different. The best-performing network for the RT prediction was the one that had 100 neurons in its hidden layer. That network yielded R² of 0.67 and RMSE of 0.21 °C, while the ANN model proposed in the present work yielded R² of 0.73 and RMSE of 0.27 °C. The major difference between these two approaches is in the fact that the presently proposed ANN model allows individual assessments, because it uses the body surface temperature as input and thus accounts for characteristics of individual animals.

The RT predictions of the ANN model for thermal stress assessment were strongly correlated with the measured RT values (94.35%), and the performance was markedly superior compared with that of the THI-based method. The THI classified 9.05% of measures as “emergency” while RT was 0%. Indeed, RT values above 40 °C were not observed, indicating that animals were not in a situation of emergency. Furthermore, unlike what occurs in the THI-based classification, the ANN-based classifier allowed individual assessments, i.e., during the same period of day, different animals from the same group were classified into different levels of thermal stress. In addition, the correspondence between the classifications of measured RTs and PRTs was better than the equivalent correspondence obtained by Sousa et al.

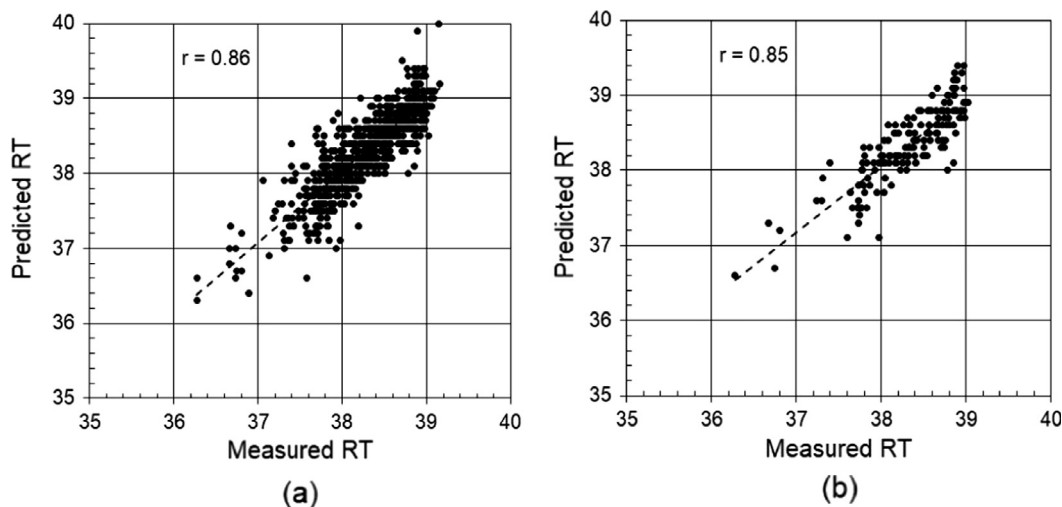


Fig. 3. Correspondence between measured and predicted rectal temperature (RT) and, for the best ANNs: (a) for the training set data; (b) for the test set data. In each plot, the points represent individual measurements, the dotted line represents the linear regression, and r represents the correlation coefficient.

Table 5

Statistical parameters of the linear regression model for rectal temperature based on the dry bulb temperature (DBT), infrared temperature (IRT), and wet bulb temperature (WBT).

	Trait	Model Parameter	Partial R ²	Model R ²
Training Data	Intercept	35.87991	–	–
	DBT	0.04289	0.4960	0.4960
	IRT Front	0.02856	0.0194	0.5154
	WBT	0.05988	0.0179	0.5333

R², coefficient of determination.

Table 6

Statistical results of the linear regression model, for the training set data and test set data.

	Training	Testing
Slope	1.00	1.02
Intercept	0.00	–0.70
Mean Error (°C)	0.28	0.28
RMSE (°C)	0.36	0.34
R ²	0.53	0.57

Table 7

Frequency distribution and coincidence (%) of data classifications using the measured and predicted rectal temperature (RT), and using the THI.

		THI				
		Normal	Alert	Danger	Emergency	Total
RT by Neural Model	Normal	31.66	43.97	15.08	8.54	99.25
	Alert	0	0.25	0	0.50	0.75
	Danger	0	0	0	0	0
	Emergency	0	0	0	0	0
	Total	31.66	44.22	15.08	9.05	100.0
Measured RT	Normal	31.66	42.71	13.07	6.78	94.22
	Alert	0	1.51	2.01	1.88	5.40
	Danger	0	0	0	0.38	0.38
	Emergency	0	0	0	0	0
	Total	31.66	44.22	15.08	9.05	100.0

(2016) (83.20%).

The good performance of the proposed ANN model was only reflected in its generalizability, which refers to the predictive performance of a model on previously unseen data. Moreover, this generalizability increased the feasibility of the proposed algorithm for

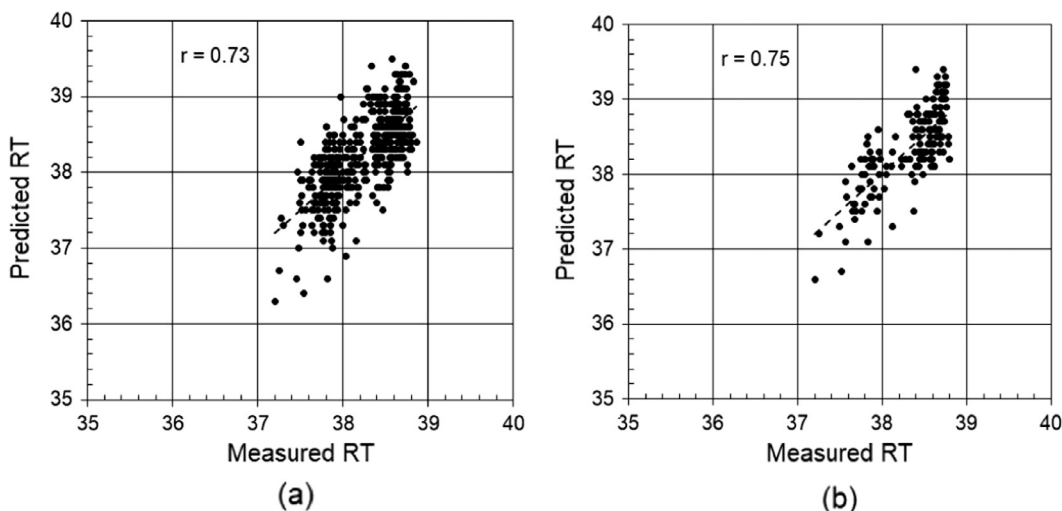


Fig. 4. Correspondence between measured and predicted rectal temperature (RT) and for the linear regression model: (a) for the training set data; (b) for the test set data. In each plot, the points represent individual measurements, the dotted line represents the linear regression, and r represents the correlation coefficient.

Table 8
Frequency distribution and agreement (%), for measurement-based and prediction-based rectal temperature (RT) classification.

		Measured RT				Total
		Normal	Alert	Danger	Emergency	
RT by Neural Model	Normal	93.97	5.03	0.25	0	99.25
	Alert	0.25	0.38	0.13	0	0.75
	Danger	0	0	0	0	0
	Emergency	0	0	0	0	0
	Total	94.22	5.40	0.38	0	100

determining the best model using the proposed iterative process that associated different hidden layer architectures with different random partitions of the dataset for training.

4. Conclusion

A method was presented for developing a model based on the neural artificial intelligence for predicting the rectal temperature of cattle based on weather (dry bulb temperature and) data and non-invasive physiological measurements of body surface temperature using. A new training approach was proposed in which one hundred neural networks were trained for each hidden layer architecture, with random partitions of the dataset, thus avoiding the problem of using non-representative data that could yield poorly generalizable models. The proposed model showed a good performance on rectal temperature prediction tasks compared with a classical regression model, and demonstrated a better capacity for persistent performance on previously unseen data. In addition, the proposed model allows to assess thermal stress conditions of individual animals, during the same period of day. In addition, the performance of the model was better than those of previously proposed comparable models. These results suggest that the proposed method is promising for development of systems for continuous, real-time, and individual assessment of animal welfare in the production system environment.

Acknowledgements

Funding for this study was provided by Sao Paulo Research Foundation (FAPESP; grant 2009/16904-0), São Paulo, SP, Brazil.

References

Brown-Brandl, T.M., Jones, D.D., Woldt, W.E., 2005. Evaluating modelling techniques for cattle heat stress prediction. *Biosyst. Eng.* 91 (4), 513–524. <http://dx.doi.org/10.1016/j.biosystemseng.2005.04.003>.

Burfeind, O., Suthar, V.S., Heuwieser, W., 2012. Effect of heat stress on body temperature in healthy early postpartum dairy cows. *Theriogenology* 78 (9), 2031–2038. <http://dx.doi.org/10.1016/j.theriogenology.2012.07.024>.

Collier, R.J., Dahl, G.E., VanBaale, M.J., 2006. Major advances associated with environmental effects on dairy cattle. *J. Dairy Sci.* 89 (4), 1244–1253. [http://dx.doi.org/10.3168/jds.S0022-0302\(06\)72193-2](http://dx.doi.org/10.3168/jds.S0022-0302(06)72193-2).

Dikmen, S., Hansen, P.J., 2009. Is the temperature-humidity index the best indicator of heat stress in lactating dairy cows in a subtropical environment? *J. Dairy Sci.* 92 (1), 109–116. <http://dx.doi.org/10.3168/jds.2008-1370>.

Eigenberg, R.a., Brown-Brandl, T.M., Nienaber, J.A., Hahn, G.L., 2005. Dynamic response indicators of heat stress in shaded and non-shaded Feedlot Cattle, Part 2: predictive

relationships. *Biosyst. Eng.* 91 (1), 111–118. <http://dx.doi.org/10.1016/j.biosystemseng.2005.02.001>.

Gaughan, J.B., Mader, T.L., 2013. Body temperature and respiratory dynamics in unshaded beef cattle. *Int. J. Biometeorol.* 1–8. <http://dx.doi.org/10.1007/s00484-013-0746-8>.

Hernandez-Julio, Y.F., Yanagi Jr., T., Avila Pires, M. de F., Lopes, M.A., de Lima, R.R., 2014. Models for prediction of physiological responses of holstein dairy cows. *Appl. Artif. Intell.* 28(8), 766–792. <http://doi.org/10.1080/08839514.2014.952919>.

Huang, Y., Lan, Y., Thomson, S.J., Fang, A., Hoffmann, W.C., Lacey, R.E., 2010. Development of soft computing and applications in agricultural and biological engineering. *Comput. Electron. Agric.* 71 (2), 107–127. <http://dx.doi.org/10.1016/j.compag.2010.01.001>.

Kessel, L., Johnson, L., Arvidsson, H., Larsen, M., 2010. The relationship between body and ambient temperature and corneal temperature. *Invest. Ophthalmol. Vis. Sci.* 51, 6593–6597. <http://dx.doi.org/10.1167/iovs.10-5659>.

Kolb, E., 1987. *Lehrbuch der Physiologie der Haustiere*. Trans. Waldir Gandolfi. Guanabara-Koogan, Rio de Janeiro.

Mader, T., 2006. Environmental factors influencing heat stress in feedlot cattle. *J. Anim.* 712–719. Retrieved from. <<http://www.journalofanimalscience.org/content/84/3/712.short>>.

Mader, T.L., Griffin, D., 2015. Management of cattle exposed to adverse environmental conditions. *Veter. Clin. North Am.: Food Anim. Pract.* 31 (2), 247–258. <http://dx.doi.org/10.1016/j.cvfa.2015.03.006>.

Martello, L.S., da Luz e Silva, S., Gomes, R.C., Corte, R.R.P.S., Leme, P.R., 2015. Infrared thermography as a tool to evaluate body surface temperature and its relationship with feed efficiency in *Bos indicus* cattle in tropical conditions. *Int. J. Biometeorol.* <http://dx.doi.org/10.1007/s00484-015-1015-9>.

Mccafferty, D.J., 2007. The value of infrared thermography for research on mammals: previous applications and future directions. *Mammal Rev.* 37 (3), 207–223. <http://dx.doi.org/10.1111/j.1365-2907.2007.00111.x>.

Metzner, M., Sauter-Louis, C., Seemueller, A., Petzl, W., Klee, W., 2014. Infrared thermography of the udder surface of dairy cattle: characteristics, methods, and correlation with rectal temperature. *Vet. J.* 199 (1), 57–62. <http://dx.doi.org/10.1016/j.tvjl.2013.10.030>.

Montanholi, Y.R., Odongo, N.E., Swanson, K.C., Schenkel, F.S., McBride, B.W., Miller, S.P., 2008. Application of infrared thermography as an indicator of heat and methane production and its use in the study of skin temperature in response to physiological events in dairy cattle (*Bos taurus*). *J. Therm. Biol.* 33 (8), 468–475. <http://dx.doi.org/10.1016/j.jtherbio.2008.09.001>.

Montanholi, Y.R., Swanson, K.C., Schenkel, F.S., McBride, B.W., Caldwell, T.R., Miller, S.P., 2009. On the determination of residual feed intake and associations of infrared thermography with efficiency and ultrasound traits in beef bulls. *Livestock Sci.* 125 (1), 22–30. <http://dx.doi.org/10.1016/j.livsci.2009.02.022>.

Schaefer, A.L., Cook, N.J., Bench, C., Chabot, J.B., Colyn, J., Liu, T., Webster, J.R., 2012. The non-invasive and automated detection of bovine respiratory disease onset in receiver calves using infrared thermography. *Res. Vet. Sci.* 93 (2), 928–935. <http://dx.doi.org/10.1016/j.rvsc.2011.09.021>.

Scharf, B., Leonard, M.J., Weaver, R.L., Mader, T.L., Hahn, G.L., Spiers, D.E., 2011. Determinants of bovine thermal response to heat and solar radiation exposures in a field environment. *Int. J. Biometeorol.* 55 (4), 469–480. <http://dx.doi.org/10.1007/s00484-010-0360-y>.

Shao, B., Xin, H., 2008. A real-time computer vision assessment and control of thermal comfort for group-housed pigs. *Comput. Electron. Agric.* 62 (1), 15–21. <http://dx.doi.org/10.1016/j.compag.2007.09.006>.

Da Silva, R.G., Morais, D.A.E.F., Guilhermino, M.M., 2007. Evaluation of thermal stress indexes for dairy cows in tropical regions. *Revista Brasileira de Zootecnia* 36 (4), 1192–1198. <http://dx.doi.org/10.1590/S1516-35982007000500028>.

Sousa, R.V., Canata, T.F., Leme, P.R., Martello, L.S., 2016. Development and evaluation of a fuzzy logic classifier for assessing beef cattle thermal stress using weather and physiological variables. *Comput. Electron. Agric.* 127 (1), 176–183. <http://dx.doi.org/10.1016/j.compag.2016.06.014>.

Taylor, C.R., Robertshaw, D., Hofmann, R., 1969. Thermal panting: a comparison of wildebeest and zebu cattle. *Am. J. Physiol.* 217, 907–910.

Thom, E.C., 1959. The discomfort index. *Weatherwise* 12, 57–59.

Wathes, C.M., Kristensen, H.H., Aerts, J.M., Berckmans, D., 2008. Is precision livestock farming an engineer's daydream or nightmare, an animal's friend or foe, and a farmer's panacea or pitfall? *Comput. Electron. Agric.* 64 (1), 2–10. <http://dx.doi.org/10.1016/j.compag.2008.05.005>.

Weschenfelder, A.V., Saucier, L., Maldague, X., Rocha, L.M., Schaefer, A.L., Fauticano, L., 2013. Use of infrared ocular thermography to assess physiological conditions of pigs prior to slaughter and predict pork quality variation. *Meat Sci.* 95 (3), 616–620. <http://dx.doi.org/10.1016/j.meatsci.2013.06.003>.